Data-driven time-frequency analysis of seismic data using regularized nonstationary autoregression

Guoning Wu[*1,2], *Sergey Fomel*[2], *Yangkang Chen*[3]
1. China University of Petroleum,Beijing. 2. The University of Texas at Austin. 3. Oak Ridge National Laboratory

SUMMARY

Time-frequency decomposition can capture the nonstationary character of seismic data. In this paper, we propose a new method of time-frequency analysis based on regularized nonstationary autoregression coupled with Hilbert-Huang spectrum (RNARHHS). RNARHHS is an empirical-mode-decomposition like method but uses regularized nonstationary autoregression to construct its intrinsic mode functions (IMFs). Examples of synthetic and field seismic data show that this method achieves high time-frequency resolution and can detect low-frequency anomalies.

INTRODUCTION

Time-frequency (TF) analysis maps an 1D time signal into 2D time and frequency domain, which can capture the nonstationary character of seismic data. TF analysis is a fundamental tool for seismic data analysis and geological interpretation (Castagna et al., 2003; Reine et al., 2009; Chen et al., 2014; Liu et al., 2016). Conventional TF methods, such as short time Fourier transform (STFT) (Cohen, 1989), wavelet transform (WT) (Mallat, 1989) and S transform (ST) (Stockwell et al., 1996) are under the control of Gabor uncertainty principle, which states that we cannot simutaneously locate the exact time and frequency of a signal (Mallat, 2009). Moreover, STFT, WT and ST are using a windowing process, which may bring smearing and leakage. Smearing means the widening of main lobe, and leakage corresponds to sidelobe leakage (Tary et al., 2014). Therefore spurious frequencies are often generated, which blur the real ones. In recent years, many new methods were proposed such as matching pursuit (Mallat and Zhang, 1993), basis pursuit (Chen et al., 1998), empirical mode decomposition (EMD) (Huang et al., 1998; Chen and Fomel, 2015). The EMD method decomposes a signal into symmetric, narrow-band waveforms called intrinsic mode functions (IMF) to compress artificial (or spurious) spectra caused by sudden changes and therefore to improve the TF resolution (Han and van der Baan, 2013). However, the EMD method also suffers from mode mixing and splitting problems. In order to solve the above problems, alternative methods were developed based on EMD: ensemble empirical mode decomposition (EEMD) (Wu and Huang, 2009), complete ensemble empirical decomposition (CEEMD) (Torres et al., 2011). However, these two methods, like the EMD, are still ”empirical” because their sketchy mathematical justifications. The synchrosqueezing wavelet transform (Daubechies et al., 2011) captures the philosophy of EMD, but uses a different method in constructing its components to provide a rigorous mathematical framework.

Fomel (2013) proposed the nonstationary Prony method based on regularized nonstationary autoregression (RNAR). RNAR was previously applied to regularization (Liu and Fomel, 2011) and denoising (Liu et al., 2012; Yang et al., 2015). The method decomposes a signal into components with controlled smoothness of amplitudes and frequencies like the EMD method, but uses Prony method to extract the components instead. However, the components do not clearly correspond to frequencies, and thus the method does not clearly define a real TF map but a ”time-component” (TC) map.

In this paper, we propose to incorporate Hilbert-Huang transform into Fomel's method. By doing this we are able to obtain a real TF map instead of a TC map of the input signal. Also, the regularization process makes the components more continuous compared with EMD's IMFs. In addition, the nonstationary regularization makes the method more localized, and more suitable for nonsationary signal analysis. Therefore, this method can improve the TF resolution of the input signal compared with the map of the EMD. After we obtain the decomposed components, we use Hilbert-Huang tansform to compute the spectrum, we additionally smooth the TF map to eliminate the irregularness coupled with the Hilbert-Huang spectrum.

Synthetic and real data tests confirm that the proposed method has higher resolution than the EMD method, and can detecting subtle low frequency anomalies.

THEORY

EMD

EMD is a data-driven method, and it is a powerful tool for nonstationary signal analysis (Huang et al., 1998). This method decomposes a signal into slowly varing time dependent amplitudes and phases components called IMFs. The TF map of the input signal is the computation of the instantaneous frequency for its each IMF (Han and van der Baan, 2013). If $s(t)$ is the input signal, the EMD decomposition can be written as

$$s(t) = \sum_{k=1}^{K} s_k(t) = \sum_{k=1}^{K} A_k(t)\cos(\phi_k(t)), \tag{1}$$

where $A_k(t)$ measures amplitude modulation, and $\phi_k(t)$ measures phase oscillation. Each $s_k(t)$ called IMF, which has a narrow-band waveform and an instantaneous frequency that is smooth and positive. The EMD is powerful, but its mathematical theory is sketchy.

Prony method

Prony method can extract damped complex exponential signals (or sinusoids) from a given signal, by solving a set of linear equations (Prony, 1795; Peter and Plonka, 2013; Mitrofanov and Priimenko, 2015). This allows for estimation of frequency, amplitude and phase of a signal. Assume we want to slove the problem

$$x[n] = \sum_{k=1}^{M} A_k e^{(\alpha_k + j\omega_k)(n-1)\Delta t + j\phi_k}, \quad (2)$$

if we let $h_k = A_k e^{j\phi_k}, z_k = e^{(\alpha_k + j\omega_k)\Delta t}$, we derive the concise form

$$x[n] = \sum_{k=1}^{M} h_k z_k^{n-1}. \quad (3)$$

The M equations of above (3) can be expressed in matrix form as

$$\begin{bmatrix} z_1^0 & z_2^0 & \cdots & z_M^0 \\ z_1^1 & z_2^1 & \cdots & z_M^1 \\ \vdots & \vdots & & \vdots \\ z_1^{M-1} & z_2^{M-1} & \cdots & z_M^{M-1} \end{bmatrix} \begin{bmatrix} h_1 \\ h_2 \\ \vdots \\ h_M \end{bmatrix} = \begin{bmatrix} x[1] \\ x[2] \\ \vdots \\ x[M] \end{bmatrix}. \quad (4)$$

The $z_k, k = 1, 2, \cdots, M$ can be found by solving a polynomial of the form below

$$F(z) = \prod_{k=1}^{M} (z - z_k), \quad (5)$$

the equation can be written in the form

$$F(z) = a_0 z^M + a_1 z^{M-1} + \cdots + a_{M-1} z + a_M. \quad (6)$$

The coefficients of the polynomial can be obtain by solving the following equation

$$\sum_{m=0}^{M} a_m x[n-m] = 0. \quad (7)$$

If $z_k, k = 1, 2, \cdots, M$ are obtained, then we can use equation (4) to compute $h_k, k = 1, 2, \cdots, M$

Nonstationary Prony method

The equation (7) can be rewritten as

$$\sum_{m=1}^{M} \hat{a}_m x[n-m] = x[n]. \quad (8)$$

If the $\hat{a}_m$s in equation (8) are time dependent, then we have

$$\sum_{m=1}^{M} \hat{a}_m[n] x[n-m] = x[n], \quad (9)$$

which is underdetermined. Therefore, we can apply shaping regularization (Fomel, 2007, 2009) to regularize the problem, and obtain

$$\hat{a} = F^{-1} d, \quad (10)$$

where $\hat{a}$ is a vector composed of $\hat{a}_m[n]$, the elements of vector d are $d_i[n] = S[x_i^*[n] x[n]]$, where $x_i[n] = x[n-i]$, and S is the shaping operator. The elements of matrix F are

$$F_{ij}[n] = \sigma^2 \delta_{ij} + S[x_i^*[n] x_j[n] - \sigma^2 \delta_{ij}], \quad (11)$$

where σ is the regularization parameter.

The nonstationary Prony method (Fomel, 2013) can be summarized as follows:

1. Using equation (10), we can obtain the time dependent polynomial coefficients $\hat{a}_m[n], m = 1, 2, \cdots, M$.
2. At each instant, write a polynomial of the form
$$F(z) = z^M + \hat{a}_1[n] z^{M-1} + \cdots + \hat{a}_M[n]. \quad (12)$$
3. Find the roots $\hat{z}_m[n], m = 1, 2, \cdot, M$ of the above polynomial. The instantaneous frequency of each different component is derived from the following equation
$$f_m[n] = \Re \left[\arg \left(\frac{\hat{z}_m[n]}{2\pi \Delta t} \right) \right]. \quad (13)$$
4. From the instantaneous frequency, we compute the local phase accroding to the following equation
$$\Phi_m[n] = 2\pi \sum_{k=0}^{n} f_m[k] \Delta t. \quad (14)$$
5. Finally, solving the following equation by using the regularized nonstationary regression method
$$x[n] = \sum_{m=1}^{M} \hat{A}_m[n] e^{j\Phi_m[n]} = \sum_{m=1}^{M} c_m[n]. \quad (15)$$
These $c_m[n]$s like the IMFs of EMD, are narrow-band signals.

After we decompose the input signal into narrow-band components, we can calculate the instantaneous frequency of each component by using Hilbert-Huang transform. Therefore, we can derive the TF representation of the input signal.

EXAMPLES

We use synthetic signals and real field data to test the proposed method.

Synthetic signal

We first use a simple synthetic signal to test the proposed method. Figure 1 is a synthetic signal from Hou and Shi (2013). Figure 2(a) shows the signal has three components. Figure 2(b) and Figure 2(c) show components extracted respectively by EMD and RNAR. From the figures, we see that RNAR method accurately identifies the three components that the signal has. The components derived by RNAR method are more continuous in amplitudes and frequencies compared with those obtained by the EMD method.

We use the proposed method to extract the TF map of the above synthetic signal (Figure 1). Figure 3(a) is the TF map of local time frequency method (LTFM) (Liu et al., 2011), Figure 3(b) is the TF map of the EMD method and Figure 3(c) is the TF map of the proposed method. The TF map of the EMD method has higher resolution than the TF map of LTFM. However, the TF map of the EMD is discontinuous because the Hilbert-Huang transform is highly susceptible to discontinuities of the decomposed components. The TF map of the proposed method is much better than the TF map of EMD, and the energies are concentrated in the instantaneous frequencies locations of the input signal.

2D seismic data

The second application is a 2D field seismic data (Figure 4(a)). Figure 4(b) is the 60 Hz slice of LTFM. Figure 5(a) and Figure 5(b) correspond to 30Hz and 60 Hz slices of the proposed method for the input data. Figure 5(c) and Figure 5(d) correspond to the smoothed 30Hz and 60Hz slices of the proposed method for the input data. Here we use a 2D, 3-points length triangle operator to smooth the TF map of the input signal. From the above figures, we see that the proposed method has higher resolutin than LTFM but with some discontinuities coupled with Hilbert-Huang transform. The smoothing process eliminates the discontinuities in some degree at the expense of resolution decrease. From the figures, we also see that there is a low frequency anomaly in the upper left part of the data section, which may correspond to gas presentation.

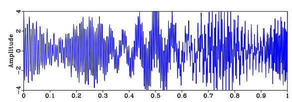

Figure 1: Synthetic signal.

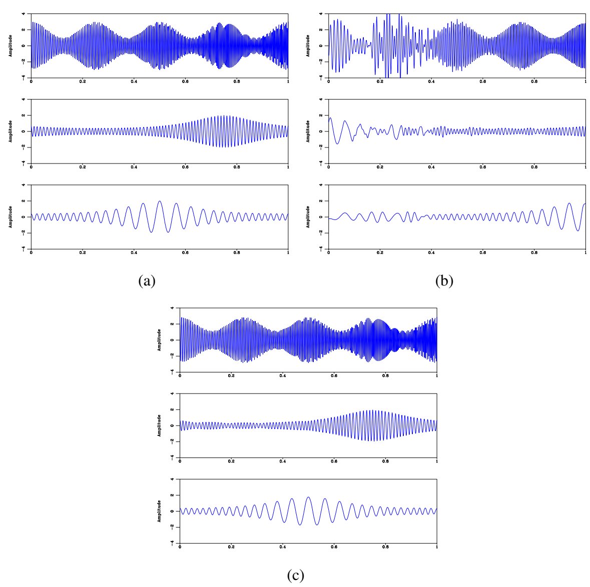

Figure 2: (a) Components making the synthetic signal in Figure 1. (b) Components derived by EMD. (c) Components derived by RNAR.

We then use another field data example to show the TF analysis performance using the proposed approach. The dataset is shown in Figure 6. Figure 7 shows the full TF decomposition result using the proposed approach. The main panel shows a constant frequency slice. The panel on the right hand side shows a TF map of 150th trace. It is obvious that each trace is decomposed into three main oscillating components, each of which has a smoothly variable instantaneous frequency. The TF decomposition is of high-resolution, which facilitates a high-resolution delineation of the subsurface properties including structural and stratigraphic features. We selected three constant frequency slices and show them in Figure 8. Because of the high-resolution properties of the proposed approach, we can see some interesting phenomena with respect to the frequency components variations. For example, we can see a strong absorption of high-frequency components around 0.5s and 125th trace. The absorption layer is very thin and cannot be observed from the original amplitude map. From the constant frequency slices, we can see such an absorption layer is just between two reflection layers, as can be see from 60 Hz slide in Figure 8(c). This absorption layer might indicate a thin-bed reservoir. Another very abnormal phenomenon is the abnormal low-frequency contents around 1.75s and 125th trace in Figure 8(b). If we correlate the anomaly with the original amplitude profile, it may also indicate a potential reservoir.

CONCLUSION

We proposed to compute the TF map of the input signal based on RNAR coupled with Hilbert-Huang spectrum (HHS); we utilized triangular smoothness to compress the fluctuation of the HHS. The proposed method is an EMD-like method but with nonstationary Prony method to construct its components. The components derived are with controlled smoothness of amplitudes and frequencies with which we can obtain higher resolution TF map compared with the EMD method. Potential application include inversion, Q estimation, denoising, etc.

ACKNOWLEDGMENTS

We would like to thank Zhiguang Xue, and Junzhe Sun for their constructive suggestions. The first author thanks China University of Petroleum-Beijing for supporting his visiting to the Bureau of Economic Geology at UT Austin.

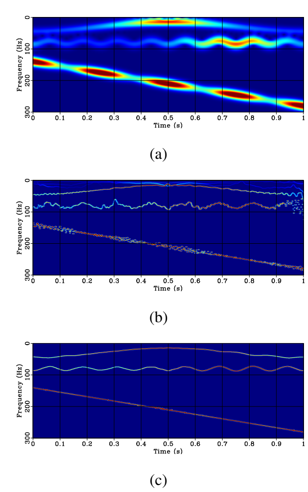

Figure 3: (a) TF of LTFM. (b) TF of EMD. (c) TF of the proposed method.

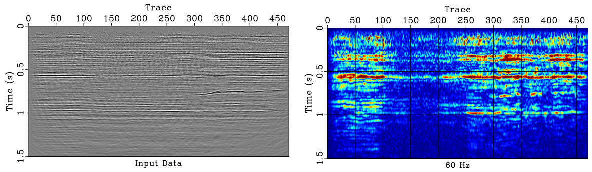

(a) (b)

Figure 4: (a) 2D seismic data section. (b) 60Hz slice of LTFM.

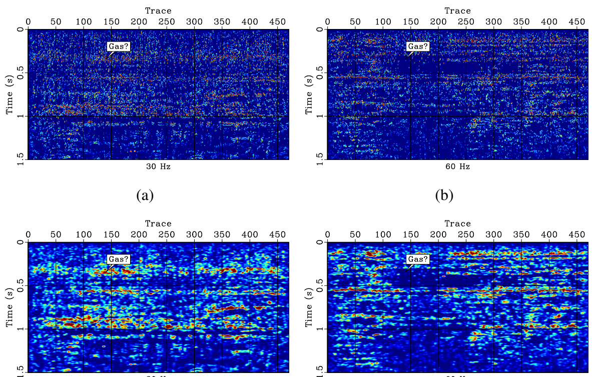

(a) (b) (c) (d)

Figure 5: (a) 30Hz slice of proposed method. (b) 60Hz slice of proposed method. (c) Smoothed 30Hz slice of proposed method. (d) Smoothed 60Hz slice of proposed method.

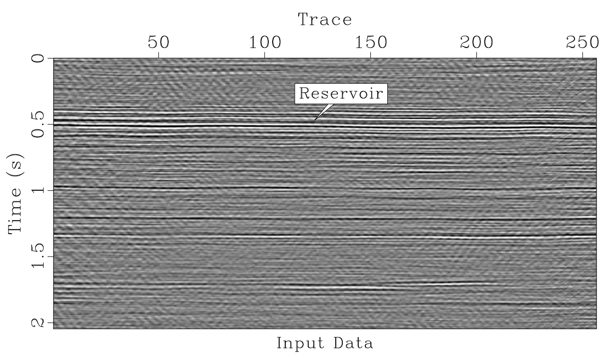

Figure 6: Post-stack field dataset.

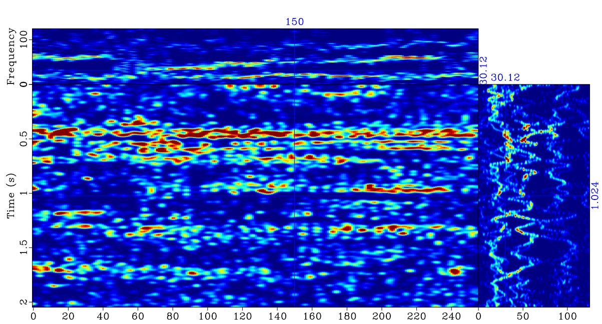

Figure 7: Time-frequency decomposition result of the second field data example.

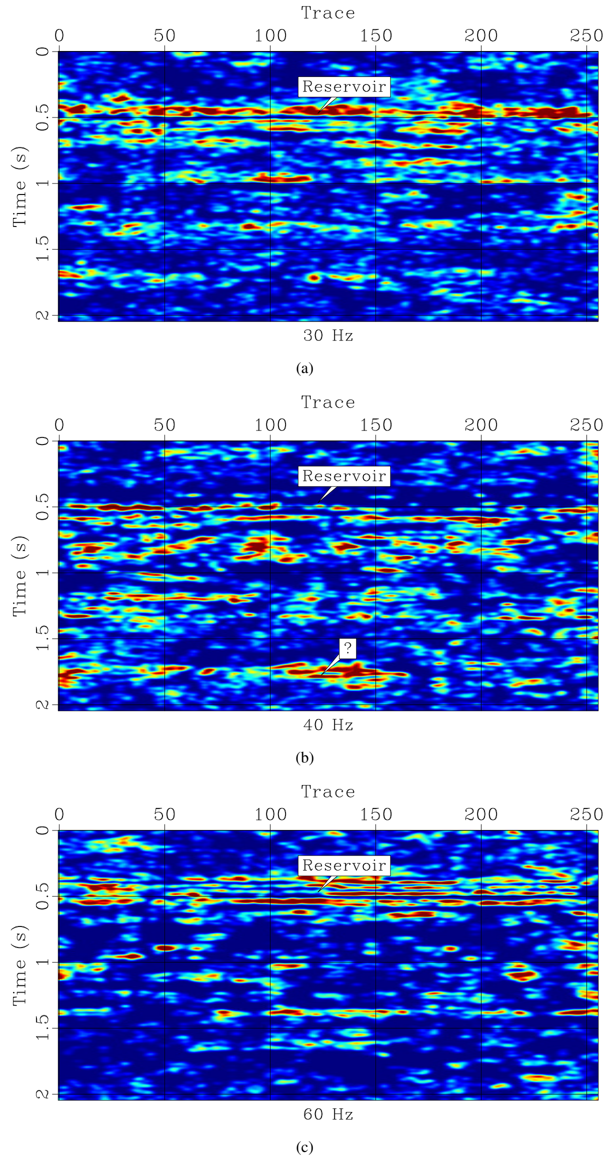

(a) (b) (c)

Figure 8: (a) Smoothed 30Hz slice of proposed method. (b) Smoothed 40Hz slice of proposed method. (c) Smoothed 60Hz slice of proposed method.

EDITED REFERENCES

Note: This reference list is a copyedited version of the reference list submitted by the author. Reference lists for the 2016 SEG Technical Program Expanded Abstracts have been copyedited so that references provided with the online metadata for each paper will achieve a high degree of linking to cited sources that appear on the Web.

REFERENCES

Castagna, J., S. Sun, and R. W. Siegfried, 2003, Instantaneous spectral analysis: Detection of low-frequency shadows associated with hydrocarbons: The Leading Edge, **22**, 120–127, http://dx.doi.org/10.1190/1.1559038.

Chen, S. S., D. L. Donoho, and M. A. Saunders, 1998, Atomic decompositon by basis pursuit: SIAM.

Chen, Y., and S. Fomel, 2015, EMD-seislet transform: 85th Annual International Meeting, SEG, Expanded Abstracts, 4775–4778, http://dx.doi.org/10.1190/segam2015-5923901.1.

Chen, Y., T. Liu, X. Chen, J. Li, and E. Wang, 2014, Time-frequency analysis of seismic data using synchrosqueezing wavelet transform: Journal of Seismic Exploration, **23**, 303–312.

Cohen, L., 1989, Time-frequency distributions — A review: Proceedings of the IEEE, **77**, 941–981, http://dx.doi.org/10.1109/5.30749.

Daubechies, I., J. Lu, and H. T. Wu, 2011, Synchrosqueezed wavelet transforms: An empirical mode decomposition-like tool: Applied and Computational Harmonic Analysis, **30**, 243–261, http://dx.doi.org/10.1016/j.acha.2010.08.002.

Fomel, S., 2007, Shaping regularization in geophysical-estimation problems: Geophysics, **72**, no. 2, R29–R36, http://dx.doi.org/10.1190/1.2433716.

Fomel, S., 2009, Adaptive multiple subtraction using regularized nonstationary regression: Geophysics, **74**, no. 1, V25–V33, http://dx.doi.org/10.1190/1.3043447.

Fomel, S., 2013, Seismic data decomposition into spectral components using regularized nonstationary autoregression: Geophysics, **78**, no. 6, O69–O76, http://dx.doi.org/10.1190/geo2013-0221.1.

Han, J., and M. van der Baan, 2013, Empirical mode decomposition for seismic time-frequency analysis: Geophysics, **78**, no. 2, O9–O19, http://dx.doi.org/10.1190/geo2012-0199.1.

Hou, T. Y., and Z. Shi, 2013, Data-driven time-frequency analysis: Applied and Computational Harmonic Analysis, **35**, 284–308, http://dx.doi.org/10.1016/j.acha.2012.10.001.

Huang, N. E., Z. Shen, S. R. Long, M. C. Wu, H. H. Shih, Q. Zheng, N.-C. Yen, C. C. Tung, and H. H. Liu, 1998, The empirical mode decomposition and the Hilbert spectrum for nonlinear and non-stationary time series analysis: Proceeding of the Royal Society of London Series A, **454**, 903–995, http://dx.doi.org./10.1098/rspa.1998.0193.

Liu, W., S. Cao, and Y. Chen, 2016, Seismic time-frequency analysis via empirical wavelet transform: IEEE Geoscience and Remote Sensing Letters, **13**, no. 1, 28–32, http://dx.doi.org/10.1109/LGRS.2015.2493198.

Liu, G., X. Chen, J. Du, and K. Wu, 2012, Random noise attenuation using f -x regularized nonstationary autoregression: Geophysics, **77**, no. 2, V61–V69, http://dx.doi.org/10.1190/geo2011-0117.1.

Liu, Y., and S. Fomel, 2011, Seismic data interpolation beyond aliasing using regularized nonstationary autoregression: Geophysics, **76**, no. 5, V69–V77, http://dx.doi.org/10.1190/geo2010-0231.1.

Liu, G., S. Fomel, and X. Chen, 2011, Time-frequency analysis of seismic data using local attributes: Geophysics, **76**, no. 6, 23–P34, http://dx.doi.org/10.1190/geo2010-0185.1.

Mallat, S. G., 1989, A theory for multiresolution signal decomposition: The wavelet representation: IEEE Transactions on Pattern Analysis and Machine Intelligence, **11**, 674–693, http://dx.doi.org/10.1109/34.192463.

Mallat, S., 2009, A wavelet tour of signal processing: The sparse way: Academic Press.

Mallat, S., and Z. Zhang, 1993, Matching pursuit with time-frequency dictionaries: IEEE Transactions on Signal Processing, **41**, 3397–3415, http://dx.doi.org/10.1109/78.258082.

Mitrofanov, G., and V. Priimenko, 2015, Prony Filtering of Seismic Data: Acta Geophysics **63**, 652–678, http://dx.doi.org/10.1515/acgeo-2015-0012.
Peter, T., and G. Plonka, 2013, A generalized prony method for reconstruction of sparse sums of eigenfunctions of linear operators: Inverse Problems, **29**, 025001, http://dx.doi.org/10.1088/0266-5611/29/2/025001.
Prony, R., 1795, Essai exp Â´ rimental et analytique: Annuaire de l'Ecole Polytechnique, **1**, 24.
Reine, C., M. van der Baan, and R. Clark, 2009, The robustness of seismic attenuation measurements using fixed and variable window time-frequency transforms: Geophysics, **74**, no. 2, 123–135, http://dx.doi.org/10.1190/1.3043726.
Stockwell, R. G., L. Mansinha, and R. P. Lowe, 1996, Localization of the complex spectrum: IEEE Transactions on Signal Processing, **44**, 998–1001, http://dx.doi.org/10.1109/78.492555.
Tary, J. B., R. H. Herrera, J. Han, and M. van der Baan, 2014, Spectral estimation-what is new? what is next?: Reviews of Geophysics, **52**, 723–749, http://dx.doi.org/10.1002/2014RG000461.
Torres, M. E., M. A. Colominas, G. Schlotthauer, and P. Flandrin, 2011, A complete ensemble empirical mode decomposition with adaptive noise: IEEE, IEEE International Conference on Acoustics, Speech and Signal Processing (ICASSP), 4144–4147.
Wu, Z., and N. E. Huang, 2009, Ensemble empirical mode decomposition: A noise-assisted data analysis method: Advances in Adaptive Data Analysis, **1**, 1–41, http://dx.doi.org/10.1142/S1793536909000047.
Yang, W., R. Wang, Y. Chen, J. Wu, S. Qu, J. Yuan, and S. Gan, 2015, Application of spectral decomposition using regularized non-stationary autoregression to random noise attenuation: Journal of Geophysics and Engineering, **12**, 175–187, http://dx.doi.org/10.1088/1742-2132/12/2/175.